



ARTICLE

Experimental Study of Thermal-Hydraulic-Mechanical Coupling Behavior of High-Performance Concrete

Wei Chen^{1,*}, Wenhao Zhao¹, Yue Liang¹ and Frederic Skoczylas²

¹School of Civil Engineering, Architecture and Environment, Hubei University of Technology, Wuhan, 430068, China

²CNRS, Centrale Lille, UMR9013-LaMcube-Laboratoire de Mécanique Multiphysique et Multiéchelle, Université de Lille, Lille, F-59000, France

*Corresponding Author: Wei Chen. Email: chenwei@hbut.edu.cn

Received: 19 March 2023 Accepted: 18 April 2023 Published: 18 May 2023

ABSTRACT

The design of an underground nuclear waste disposal requires a full characterization of concrete under various thermo-hydro-mechanical-chemical conditions. This experimental work studied the characterization of coupled thermo-hydro-mechanical effects using concretes made with cement CEM I or CEM V/A (according to European norms). Uniaxial and triaxial compression under 5 MPa confining pressure tests were performed under three different temperatures ($T = 20^{\circ}\text{C}$, 50°C , and 80°C). The two concretes were dried under relative humidity (RH) to obtain a partially saturated state of approximately 70%. The results showed that the effects of water saturation and confining pressure are more important than that of temperature. Drying in high RH at different target temperatures led to an increase in uniaxial and triaxial strength but drying at 105°C had a negative effect on the strength and Young's modulus. Oven drying caused microcracking in the concrete. The microcracks deeply influenced the thermal damage to the material, affecting its mechanical behavior. The triaxial strength clearly increased due to the presence of confining pressure. Moreover, an important influence of cement type was observed on the mechanical properties; the concrete based on CEM V/A had a greater porosity than CEM I, and a finer pore structure appeared due to the presence of mineral admixtures.

KEYWORDS

Concrete; temperature; saturation; uniaxial compression; triaxial compression

1 Introduction

For proper radioactive waste management, the best option is to bury the waste in a repository consisting of underground structures that isolate it and confine the radioactivity for the time necessary for its decay [1–4]. Concrete is widely used in these structures, especially those dedicated to long-lived intermediate-level waste. In storage situations, the concrete will be subjected to different environmental conditions (thermal, hydric, mechanical, chemical) over time. In France, the French National Agency for Nuclear Waste Management (Agence Nationale pour la gestion des Déchets RadioActifs, Andra) designed and assessed the feasibility and safety of radioactive waste repositories in deep geological layers. During the initial phases (excavation, construction of the structures, installation of the packages, and closure), the processes associated with the desaturation/resaturation of the materials will have an impact on the mechanical



behavior of the concrete. Because undergrounding will cause a hydraulic discharge in the geological layer, a new state of equilibrium will then occur in the form of resaturation. These processes will influence the behavior of concrete in an underground storage site and take place over a period of several thousand to several tens of thousands of years [4]. Andra considered that intermediate-level waste is the source of thermal load, and the maximum value is close to 50°C and approximately 70°C–80°C at worst [5,6]. Therefore, studying the thermo-hydro-mechanical (THM) coupling effect is critical for repository safety.

The study of uniaxial compression behavior as a function of water saturation has shown different trends. Some authors found an improvement in strength with drying [7–9], while others found a more “random” evolution [10,11]. These different trends can be explained by the variations in the fabrication and curing methods of the samples. Burlion et al. [8] tested mortar specimens in uniaxial compression according to their water saturation state (saturated, dry, and partially saturated). The strength obtained for each specimen was related to its weight loss, giving information on its saturation state. Their results showed that desiccation can be beneficial to compressive strength. Capillary suction was proposed to explain this increase in strength with the decrease in the saturation of the material. Indeed, capillary depression was one of the causes of desiccation shrinkage. The material thus locally contracted will be more resistant than in the saturated state. The second hypothesis referred to the water gradients, causing one of the structural effects of desiccation. The non-uniformity of the water gradients between the core and the surface of the material also led to a contraction of the cementitious matrix, which resulted in improved strength.

In the literature, many studies have assessed the effect of high temperature on mechanical properties [7,12–19]. The microstructure of concrete undergoes important physicochemical modifications that influence the mechanical behavior. Different authors [7,12] have agreed that the effect of temperature generally causes a decrease in Young’s modulus, Poisson’s ratio, stress failure, and plasticity threshold. The main reason for this microstructural evolution is the shrinkage of the matrix caused by the drying and dehydration phases [15]. In addition, the increase in microcracking and porosity, the influence of the nature of the paste and the aggregates, and the differential deformations between the paste and the aggregates are affected by the drying process [16].

The mechanical behavior under triaxial compression of cement-based material has shown sensitivity to the internal humidity and confinement level [20–24]. Bazant et al. [20] showed an increase in capillary pressure, surface tensions, and disjoining pressures, which influenced the mechanical properties during the drying process. Yurtdas et al. [7] showed the evolution of the maximum deviatoric stress as a function of mass loss under triaxial compression at 15 MPa confinement. For simple compression, a better deviatoric strength is observed when the material is dry. This change in strength is explained by the fact that drying induces desiccation shrinkage by variation in capillary depression, disjunction pressures, and surface energies [20]. When the confining pressure increased, the material behavior changed from brittle to ductile. The rupture of concrete occurs with microcracking at low confining pressure, failure occurs with slight microcracking, and major macrocracks occur with high confining levels [12,21].

In short, the study of THM behavior is still fragmentary. Each of these solicitations has been studied separately from the others in terms of evolution of properties or degradation of the concrete. On the other hand, very few studies have focused on the coupling of the three stresses. In the literature, we can find studies on the effects of temperature or hygrometry on the mechanical behavior of concrete, but there are very few studies on the effect of temperature on the hygrometry of concrete and even fewer on the coupling between these three factors. Therefore, we investigate the coupling effect of water saturation, moderate temperature, and confinement on the uniaxial and triaxial mechanical properties, including axial strain, strength, and Young’s modulus, for two concretes based on CEM I and CEM V/A. This experimental work can provide useful data for designing underground storage for radioactive waste.

2 Experimental Program

2.1 Materials and Specimen Preparation

In this paper, two types of cement are used: CEM I and CEM V/A. The CEM V/A contains slag (18%–30%) and siliceous fly ash (18%–30%) in addition to clinker (40%–64%). The slag comes from the blast furnaces of foundries, and the fly ash comes from the dedusting of pulverized coal-fired boiler gases. CEM I cement is commonly called “Portland cement” and is composed of a mixture of clinker and gypsum (calcium sulfate dihydrate), whose proportions are 95% and 5%, respectively. The clinker is composed of oxides chemically combined with each other, such as lime CaO, silica SiO₂, alumina Al₂O₃, and ferrite Fe₂O₃, according to the NF EN 19–4 European Standard. Table 1 presents the proportions of the various components. The superplasticizer used is a polycarboxylic ether-based, high-range water-reducing admixture for high-performance concrete.

Table 1: Components of the concretes

Component		Quantity (kg/m ³)	
Cement	CEM I	400	
	CEM V/A		450
Sand	0–4 mm	858	800
Gravel	5–12 mm	945	984
Superplasticizer	Glenium 27 (BASF)	10	11.5
Water		171	176.3
W/C		0.43	0.39
Sample name		CI	CV

The concrete is poured into a beam (Section 15 × 15 cm and length 1 m) whose upper surface is protected by a plastic sheet to limit desiccation. After demolding, the beams are cured in water saturated with lime at 21 ± 1°C for 3 months. The process of hydration is sufficiently advanced, and the microstructure of concrete has been completely developed and finalized. For the mechanical test, cylindrical samples are used. A diameter of 37 mm and a height of 74 mm are chosen for this study to ensure that representative elemental volumes (three times the diameter of the largest aggregate, i.e., 12 mm) are available while allowing for triaxial cell testing on the same specimen geometry. The concrete beam is cored, cut, and rectified. The parallelism between the flat faces of a cylindrical specimen must be as perfect as possible to not affect the homogeneity of the compressive stress. The samples are surfaced by a grinding machine with a diamond wheel. The grinding of the specimens enables the obtaining of a good state of parallelism of the upper and lower faces.

2.2 Experimental Device

The triaxial cell shown in Fig. 1 allows for the characterization of concrete behavior under high multiaxial stresses. With a conventional triaxial cell, the piston is subjected to an upward axial force due to the presence of confining pressure. This force can be significant and must be balanced by an external axial force. On the other hand, in the self-compensated cell used in this study, the confining pressure is transmitted to a chamber in the cell cap (self-compensation chamber) whose section acting on the piston is equal to the piston section. The axial force applied on the piston is thus compensated by the one imposed in the self-compensation chamber, and any external force applied to the piston is thus transmitted axially to the specimen. Two independent pumps are used for the application of the confining

pressure and the deviator. The pumps have a maximum capacity of 60 MPa, and they can inject the fluid at a speed of 5×10^{-4} to 5 ml/min. These pumps allow the pressure to be regulated, and it is possible to control the hydraulic charge and discharge with the pumps. For the tests under temperature, the cell is placed in an oven equipped with an electronic temperature controller and a fan to homogenize the temperature inside the oven. This type of oven allows a temperature precision of $\pm 0.3^\circ\text{C}$ and maintains the whole cell at the set temperature. A data acquisition chain located outside the oven is connected to the two pressure sensors and two LVDTs to record the pressures and strain.

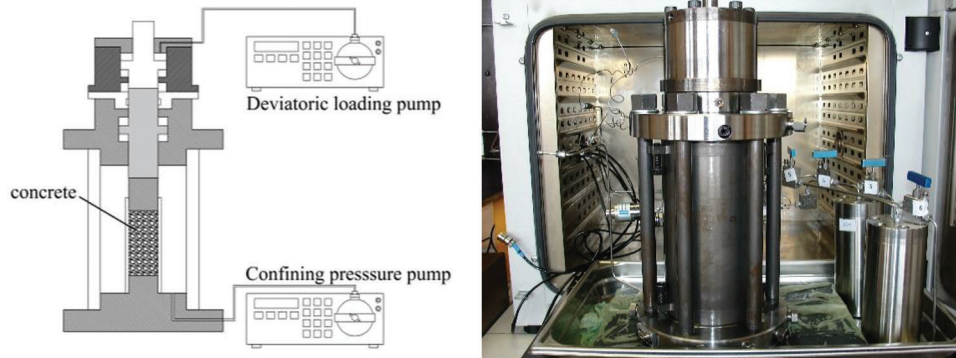


Figure 1: Triaxial cell

2.3 Experimental Procedures

Two of the parameters of concrete under investigation in this study are temperature (T) and water saturation (S_w). Three temperatures are selected: 20°C , 50°C , and 80°C , as detailed in Table 2. This choice makes it possible to study the influence of low temperatures on the behavior of concrete in a range close to that observed for applications in the underground storage of radioactive waste. Three saturation states are chosen: saturated ($S_w = 100\%$), dry ($S_w = 0\%$), and intermediate states ($S_w = 70\%$). The sample was dried in an oven at 105°C until the mass was constant in the dry state. Oven-drying at 60°C or 105°C , vacuum-drying, and freeze-drying are the most popular drying methods. A temperature of 105°C is regularly recommended as the drying temperature, however, thermally induced cracks may occur. On another hand, a moderate drying temperature may not lead to complete material de-saturation, i.e., it will not provide actual porosity and gas permeability. The saturated state of concrete is obtained at the end of 3 months of maturation in water. A climatic chamber was used to obtain 70% saturation by imposing the relative humidity at three temperatures. Before the test at 50°C and 80°C , the cell was placed in an oven, and the temperatures were achieved by low heating rates at $1^\circ\text{C}/\text{min}$ from room temperature to the target temperature and maintained for 24 h to avoid thermal shock in the samples. In order to obtain a water saturation of 70% at each temperature, a fixed relative humidity RH was imposed at 70%, sample mass variation was measured every two days during the first three weeks, and then each week until mass stabilization. To prevent carbonation, nitrogen was added in the climatic chamber after each measurement. The water saturation ($S_w\%$) is determined as:

$$S_w = \frac{m - m_d}{m_s - m_d} \times 100\% \quad (1)$$

where m is the current mass at RH-value, m_d is the dry sample mass, m_s is the saturated sample mass.

Table 2: Condition of the concrete for the compressive test

Type test	Condition of samples		
Uniaxial test and Triaxial test	3 temperatures and 3 saturation levels	Saturated state	In water at 20°C
		Partially saturated state	In a climatic chamber under three temperatures and RH = 70%
		Dry state	In an oven at 105°C

After installing the axial stress and confinement loading system at the target temperature, the confining pressure was applied by injecting oil up to 5 MPa at an injection speed of 1 mL/s, as shown in Fig. 1. The sample was axially stressed in controlled displacement at a constant speed of 2 $\mu\text{m/s}$ with loading–unloading cycles until failure. Four cycles were chosen (sample loaded at approximately 30%, 50%, 70%, and 80%–95% of the uniaxial compression strength and unloading until half of each loading). The tangent Young’s modulus for each cycle is determined as:

$$E = \frac{\Delta\sigma_{11}}{\Delta\varepsilon_{11}} \quad (2)$$

3 Results and Discussion

In this section, the experimental results obtained according to temperature, water saturation, and confinement are presented and analyzed.

3.1 Initial Characteristics of the Concretes

The porosity of concrete CI was 8.2% on average after 35 days of drying at 60°C. For concrete CV, the porosity was 12.4 on average (see Table 3). At 60°C, the relative humidity was approximately 9%, and the concrete could not attain a completely dry state. Therefore, the concretes were dried at 105°C following drying at 60°C. According to a previous study with the same formulation, the porosity is comparable. Brue et al. [25] showed that the porosity of the two concretes were 8.1% and 11.9% after drying at 60°C. Poyet [6] reported slightly greater porosities of 11.3% and 12.3% after drying at 60°C and 105°C, respectively, for concrete CEM I. Ranaivomanana et al. [26] reported that after drying at 105°C, the porosity for CEM I was 12.3% and 15.3% for CEM V.

Table 3: Properties of concrete measured at 3 months of maturation

	Drying temperature	CI	CV
Gas permeability (dry state)	105°C	4.37×10^{-18}	2.76×10^{-18}
Porosity	60°C	$8.2 \pm 0.4\%$	$12.4 \pm 0.7\%$
	105°C	$10.1 \pm 0.5\%$	$15.3 \pm 0.4\%$
Compressive strength (28-day, dry state)	60°C	62.5	55.6
Compressive strength (saturated state)		60 MPa	65 MPa
Compressive strength (dry state)	60°C	66.6 MPa	72.2 MPa
	105°C	65.07 MPa	66.1 MPa

A mercury porosimetry measurement was used to estimate the pore distribution of CI and CV, as shown in Fig. 2. In the macropore zone (1 to 100 μm), the pore entrance radius curves were identical for both

materials, meaning that their porosity was equivalent up to a pore diameter of 1 μm . Below this value, the pore entrance diameter curves allowed for distinguishing the two parts, limited by a diameter of 0.06 μm . For a diameter between 1 and 0.06 μm , CV has no or few pores, as its pore entry diameter curve does not change. In contrast, over this same range, the pore volume of CI doubles, confirming the large proportion of pores of this size in its microstructure. Below a radius of 0.06 μm , the inlet diameter curve of CV increases rapidly and that of CI tends toward a plateau. The evolution of CI indicates that it has no or few pores with a diameter of less than 0.07 μm . However, CV shows a truncated input diameter evolution due to the technical limitations of the device, suggesting that most of the pores in CV are smaller than 6 nm in diameter. The porosity distributions of CI and CV are therefore indicative of the influence of the nature of the cement used. The additions present in the CEM V/A cement induce a pozzolanic reaction, which generates a refinement in the hydrate porosity.

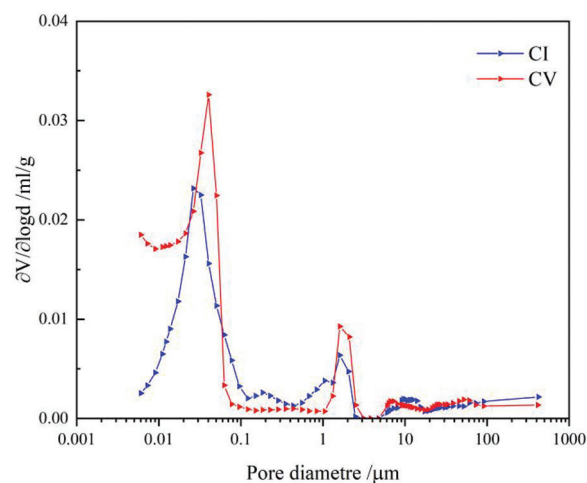


Figure 2: Distributions of pore size in concretes CI and CV

The uniaxial compressive strength test was carried out on two concretes at different states without loading and unloading cycles as initial properties. In [Table 3](#), the obtained properties of the two concretes are summarized. The porosity shows significant differences between the different compositions. The increase in porosity is caused by the evaporation of the free water between 60°C and 105°C, and a variation in the pore structure of the concrete due to the elevated temperature. After 3 months the samples cured in the water achieved a higher compressive strength than that in 28 days due to the pozzolanic reaction. The cement CEM V/A is composed about 40% pozzolanic additions, which produce a densified, refined pore system and greater strength. The concrete CI had a lower compressive strength and was less porous than CV after 3 months of maturation. The maximum compressive strength was obtained for the concrete dried at 60°C. The drying effect plays an important role in compressive strength. Drying at 60°C led to more compaction of the dry concrete due to the desiccation shrinkage induced by capillary depression and leading to increased compressive strength. However, at 105°C, the drying induced the formation of microcracks to weaken the concrete.

3.2 Uniaxial Compression Behavior

[Table 4](#) lists the compressive strength and Young's modulus carried out on the two concretes with different water saturation. The stress-strain curves from the uniaxial compression test are presented in [Figs. 3](#) and [4](#). The behavior of concrete in uniaxial compression shows a classic concrete behavior: after an elastic phase, up to approximately 60 MPa (approximately 90% of the peak strength) for the two

concretes, the behavior of the material becomes nonlinear. After the elastic phase, microcracks develop rapidly and lead to material failure. The load/unload curves in the elastic phase exhibit hysteretic loops due to the viscosity of the material. The opening of loops decreases with increasing water saturation. This phenomenon relates to two aspects: on the one hand, to the friction between the lips of the microcracks during their reclosing or reopening, and on the other hand, to the movement of water in the microporous structure of the hydrated cement paste. Indeed, the hysteretic behavior is characteristic of energy dissipation in the material.

Table 4: Uniaxial strength and Young’s modulus of two concretes at different saturations and temperatures

Temperature	Concrete CI			Concrete CV		
	Saturation (%)	Strength (MPa)	Modulus (GPa)	Saturation (%)	Strength (MPa)	Modulus (GPa)
20°C	0	65.07	26.17	0	66.12	22.56
	70.86	66.28	26.34	76.06	72.77	25.14
	100	61.71	27.17	100	68.28	25.68
50°C	0	66.08	26.46	0	77.91	26.3
	71.98	68.30	28.50	74	78.66	28.00
	100	66.12	27.30	100	74.34	22.30
80°C	0	70.70	30.48	0	61.41	27.28
	69.57	65.05	29.1	76.89	65.45	27.42
	100	54.56	29.13	100	65.97	27.15

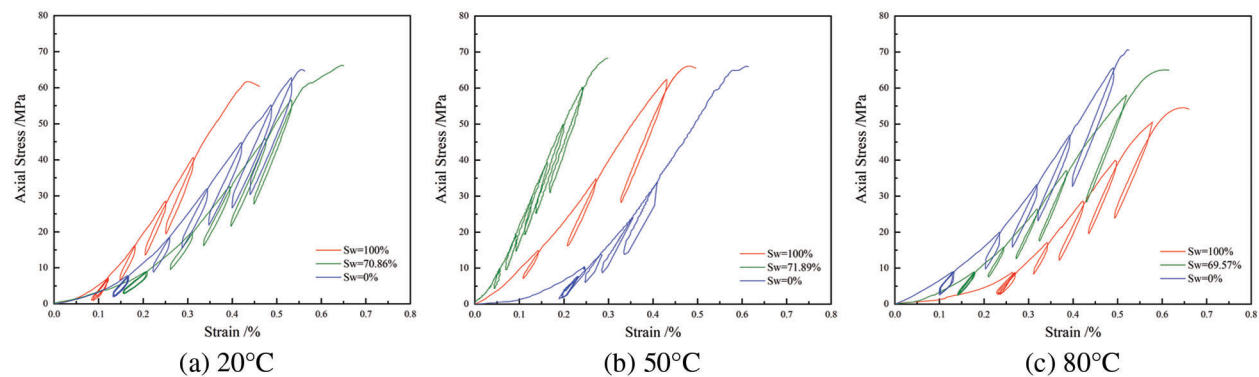


Figure 3: Axial stress vs. axial strains of concrete CI for different temperatures

Fig. 5a shows the variation in uniaxial strength for different saturations at 20°C. The strength increased by 7.4% and 5.4% when the saturation decreased from 100% to 70.86% and 0% for concrete CI and by 6.5% when the saturation decreased to 72.77 for concrete CV. The drying temperature of 105°C resulted in damage to the strength of CV, and its value was lower than that of the saturated state. According to thermogravimetric analysis (TGA), after evaporation of the free water at approximately 100°C, chemically bonded water is lost at 105°C [27,28]. The C-S-H (and aluminates) decomposes from 105°C (or 145°C) to 400°C. The decomposition peak of ettringite is at approximately 130°C. It should be noted that the temperature at the

beginning of decomposition for ettringite and C-S-H is modified in particular in the presence of liquid water [28]. Although concrete CV is globally more resistant than CI, desiccation appears more beneficial for CI. Concrete CI benefits from the influence of capillary pressure on the drying process, with a risk of microcracking, which seems lower. Concrete CV seems to be more insensitive to the effects of desiccation in terms of strength; it has a lower permeability but presents higher deformations. The developed microcracking and/or creep of CSH, induced by desiccation, leads to a lower strength gain with desiccation for CV. The concrete CV is softer than the CI. The evolution of Young's modulus can be broken down into two parts: from the saturated state, the modulus remains almost constant until the tested intermediate saturation states ($S_w = 70.86\%$ for CI, and $S_w = 76.06\%$ for CV), followed by a slight decrease to the value in the dry state (see Fig. 6). These two parts illustrate the existing competition between the effects of desiccation (capillary pressure and microcracking). As long as the increase in capillary pressure compensates for the increase in microcracking, the modulus is deeply affected. On the other hand, once the microcracking, induced by the water gradients and the effect of the rigid inclusions, becomes too important, the stiffness of the concrete decreases by 3% and 12.15%, respectively, for CI and CV. The decreases are equivalent; however, CV always presents lower Young's moduli than CI. This confirms once again that desiccation affects CV more than CI. Microcracking must therefore be more important in the microstructure of CV, despite a higher strength value.

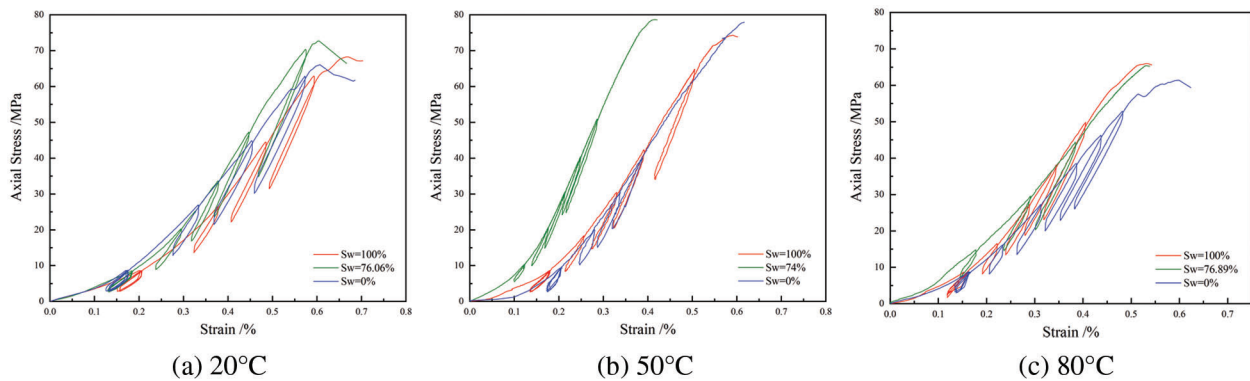


Figure 4: Axial stress vs. axial strains of concrete CV for different temperatures

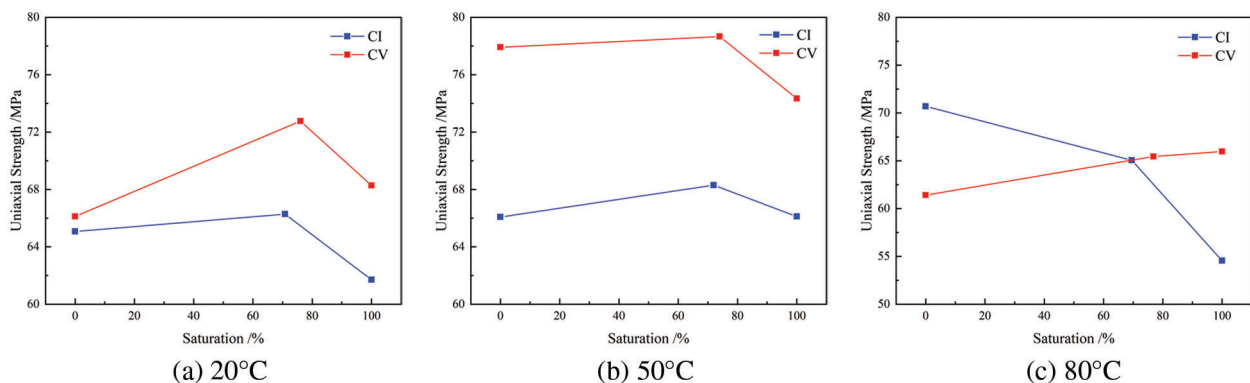


Figure 5: Variation in uniaxial strength vs. water saturation at different temperatures

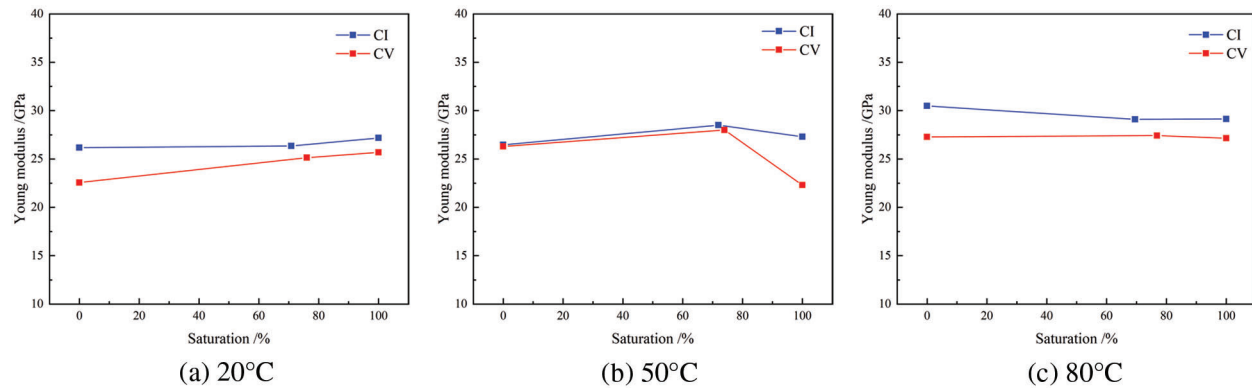


Figure 6: Variation in Young's modulus (uniaxial) vs. water saturation at different temperatures

Figs. 5b and 5c show the strength evolution of two concretes under temperatures of 50°C and 80°C as a function of water saturation. The strengths of the two concretes at 50°C were similar to those at 20°C. It appears that the saturation level ($S_w = 71.98\%$ for CI and $S_w = 74\%$ for CV) more strongly influences the strength. However, at 80°C, the strength of concretes with a partially saturated state was lower than that at 20°C. Indeed, desaturation and temperature can induce thermal and hydric gradients in the microstructure (mainly related to the thermal inertia of the concrete and its very low permeability), which can generate differential deformations, causing probable cracking. This microcracking counteracts the beneficial effect of capillary pressure. In addition, the increase in temperature leads to transport in the gas phase, which is amplified with the temperature. In the study by Brue et al. [25], it was found that the vapor pressure is multiplied by 5 at 50°C and by 20 at 80°C compared to 20°C. Locally, due to the very low permeability of concrete, an increase in vapor pressure can lead to greater pressure gradients as the temperature increases. If this pressure locally exceeds the strength of the porous structure, this leads to microcracking, which can explain the decrease in strength of partially saturated concrete at high temperatures compared to the dry state. The modulus increased slightly at 50°C and then weakly increased at 80°C. The thermal and hydric effects simultaneously influence the elastic properties; however, in our study, it seems that saturation has a more important role than moderate temperature.

3.3 Triaxial Compression Behavior

Figs. 7 and 8 show the stress-strain curves from the triaxial compression test. The influence of the confining pressure on the behavior curves is obvious. The evolution of the two concretes in the dry and saturated states was similar during the elastic phase and showed the same hysteresis loops. Compaction of the material in the dry state is induced by the confinement (pore collapse), while in the saturated state, ductility appears due to the friction between the pore water and the solid, which is caused by the application of the confinement. Thus, the compaction of the material in the dry state has a beneficial effect on the strength, leading to a greater improvement when the confinement is high. These results highlight the coupled influence of confinement and saturation state on the triaxial mechanical behavior of cementitious materials.

Table 5 and Figs. 9 and 10 show the evolution of the triaxial strength and modulus with different temperatures and water saturations. The confining pressure (5 MPa) led to an increase in the strength compared to the uniaxial strength for the same saturation state. The triaxial strength increased by 101%, 80%, and 76% at 20°C, 73%, 61%, and 52% at 50°C, and 79%, 64%, and 83% at 80°C from the dry to saturated state. Similar to that of uniaxial compression, the triaxial strength gains induced by the drying of the materials were higher for CI, despite a lower saturated strength value than for CV (see Table 5 and Fig. 9a). The effect of capillary pressure, leading to an internal prestressing of the material, was more

significant in the microstructure of CI because of its wider pore distribution. Moreover, for the same drying conditions, microcracking, induced by local and structural effects, was less developed in CEM I, which further improved the strength gain with drying compared to CV. The overpressure of interstitial water depending on saturation was higher in the triaxial case. This led to faster initiation and propagation of microcracks and thus faster failure of the specimens under triaxial compression. The confinement increased the strength of the dried specimens more than the wet specimens, which was attributed to the pressurization of the interstitial water. On the other hand, the application of confinement slowed down the effect of microcracking induced by drying. Moreover, the suction generated by drying can be assumed to be isotropic in the material, which will imply a “triaxial prestress” having a more beneficial role in the case of a triaxial compressive mechanical stress; the damage and failure processes of the material will also be delayed by this suction. At 50°C and 80°C, Young’s modulus values increased regardless of temperature. The difference between the modulus of elasticity of the two types of concrete becomes obvious due to the presence of confining pressure. Moreover, the increase in the elastic modulus of concrete CI was much larger than that of concrete CV. This further confirms that desiccation affects concrete CV more than concrete CI, and microcracking is more important in the microstructure of concrete CV, linked to a weaker paste quality in tension.

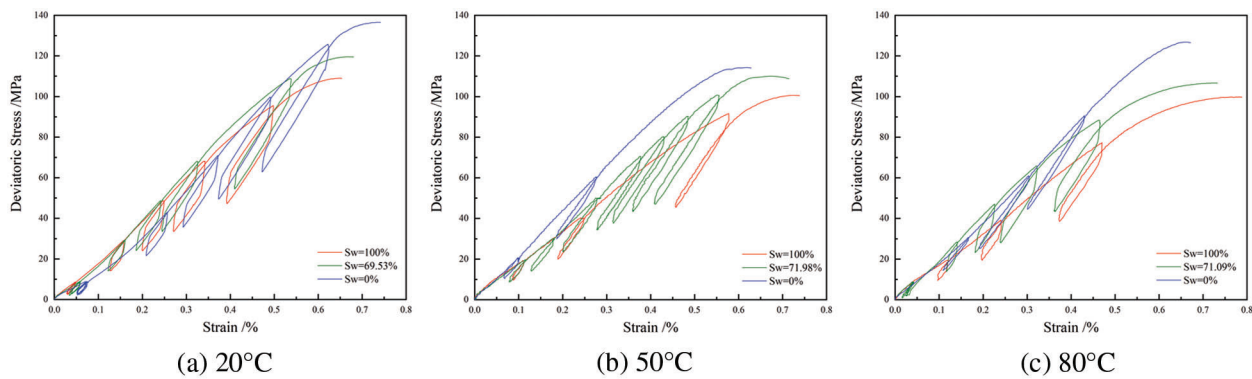


Figure 7: Axial stress vs. axial strains of concrete CI under a 5 MPa confining pressure at different temperatures

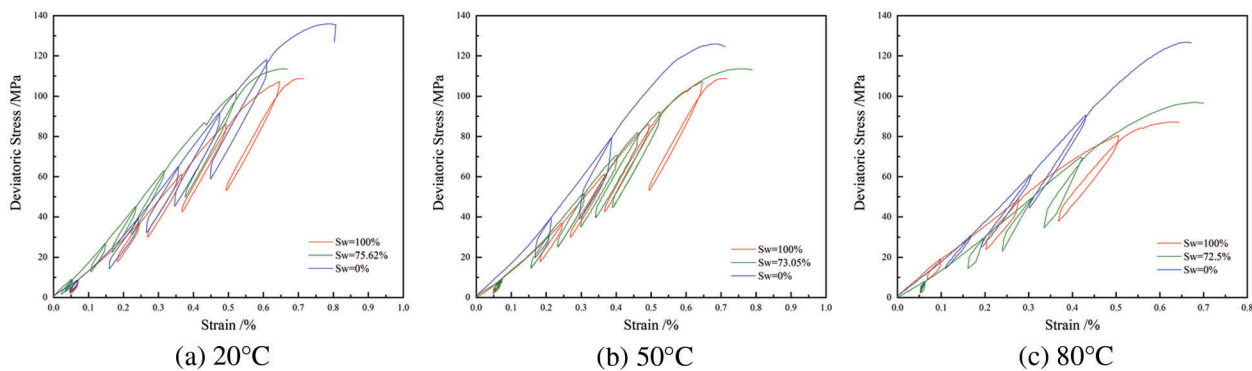


Figure 8: Axial stress vs. axial strains of concrete CV under 5 MPa confining pressure at different temperatures

Table 5: Triaxial strength and Young’s modulus of two concretes at different saturation levels and temperatures

Temperature	Concrete CI			Concrete CV		
	Saturation (%)	Strength (MPa)	Modulus (GPa)	Saturation (%)	Strength (MPa)	Modulus (GPa)
20°C	0	136.61	42.5	0	135.94	35.51
	69.53	119.59	42.04	75.62	113.67	33.96
	100	109.10	42.22	100	108.76	32.4
50°C	0	114.35	32.64	0	125.94	42.98
	71.98	110.07	34.12	73.05	113.64	32.94
	100	100.69	34.31	100	108.7	29.63
80°C	0	126.83	34.71	0	125.51	33.73
	71.09	106.71	42.57	72.5	102.58	38.17
	100	99.85	42.9	100	97.4	31.66

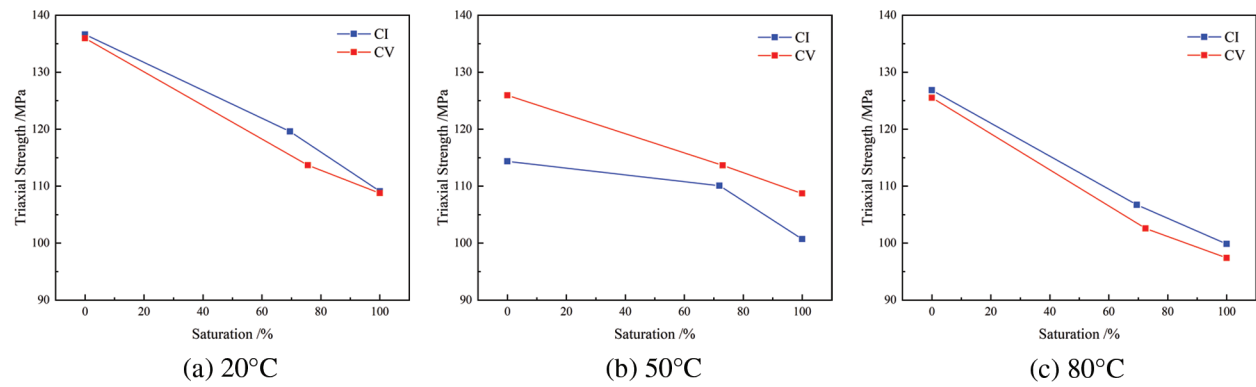


Figure 9: Variation in triaxial strength vs. water saturation at different temperatures

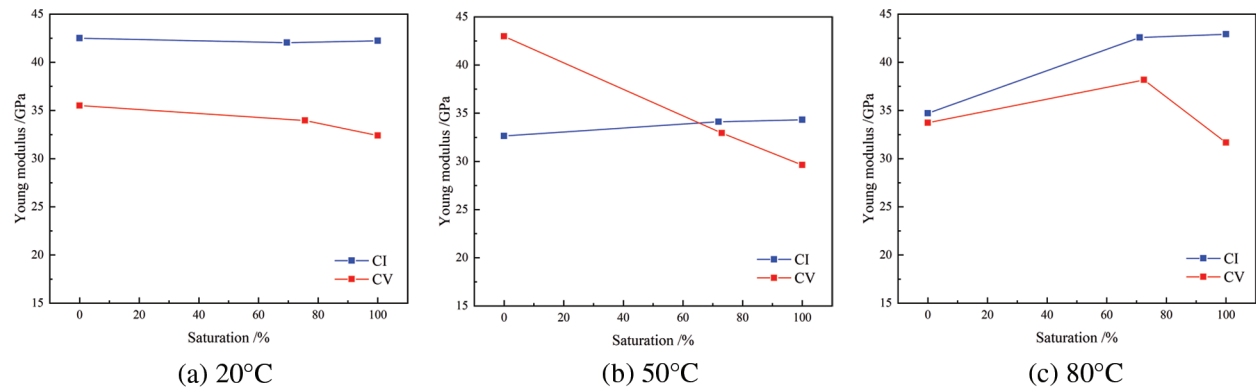


Figure 10: Variation in Young’s modulus (triaxial) vs. water saturation at different temperatures

4 Conclusions

This study highlights the coupling effect of saturation, temperature, and confinement on two different concrete materials.

The main results are summarized as follows:

1. The influence of the degree of saturation on the behavior of the concretes highlights the characteristics on which water has an influence; the microcracking and the stiffening of the concretes related to the drying before the test, the pore pressure in the concretes, and the lubrication between the solid grains. The uniaxial and triaxial compression tests allowed for an understanding of how drying influences mechanical behavior. The uniaxial and triaxial strengths of concrete increased with desiccation. Drying leads to the development of capillary depressions and water gradients, which also lead to microcracking. Thus, there is competition between stiffening and microcracking induced by desiccation.
2. The triaxial compression tests under a confining pressure of 5 MPa showed that the mechanical response becomes linear up to the elastic limit due to the closure of microcracks. The greater the confining pressure, the greater the strength, which confirms the increase in ductility of concrete in the presence of confining pressure. Young's modulus varies very little in the presence of confining pressure. Furthermore, the greater increase in strength in the triaxial case compared to the uniaxial compression is due to the presence of water in the concrete; the pore pressures in the triaxial test have more influence than the uniaxial test because of the presence of confinement, which delays the effect of the induced water microcracking. The elastic modulus of the concretes remains quasi-constant with drying in the uniaxial test. This shows significant damage after drying at 105°C and confirms a competitive effect between stiffening and damage.
3. The thermo-hydro-mechanical coupling on the mechanical properties does not show a clear effect of temperature; the elastic parameters are comparable in the range of measurement (50°C and 80°C). In the triaxial case, the results are opposite; the Young's modulus of the dry concrete increases slightly compared to the saturated and partially saturated concretes at 20°C and 50°C, which is attributed to confinement preventing the propagation of microcracking. It appears that it is the confinement pressure and drying that generate a variation in the elastic parameters.

Funding Statement: This paper was supported by the National Natural Science Foundation of China (Grant No. 51709097).

Conflicts of Interest: The authors declare that they have no conflicts of interest to report regarding the present study.

References

1. Derek Martin, C., Lanyon, G. M., Blümling, P., Mayor, J. C. (2003). The excavation disturbed zone around a test tunnel in the opalinus clay. *European Commission CLUSTER Conference*, pp. 121–125. Luxembourg.
2. Bossart, P., Meier, P. M., Moeri, A., Trick, T., Mayor, J. C. (2002). Geological and hydraulic characterisation of the excavation disturbed zone in the opalinus clay of the mont terri rock laboratory. *Engineering Geology*, 66(1–2), 19–38. [https://doi.org/10.1016/S0013-7952\(01\)00140-5](https://doi.org/10.1016/S0013-7952(01)00140-5)
3. Bossart, P., Trick, T., Meier, P. M., Mayor, J. C. (2004). Structural and hydrogeological characterisation of the excavation-disturbed zone in the opalinus clay (Mont terri project, Switzerland). *Applied Clay Science*, 26(1–4), 429–448. <https://doi.org/10.1016/j.clay.2003.12.018>
4. Plas, F., Wendling, J. (2007). The geological research in France-the dossier 2005 argile. *MRS Online Proceedings Library*, 985(1), 1301.

5. ANDRA, Dossier (2005). Référentiel des matériaux d'un stockage de déchets à haute activité et à vie longue, internal report (in French). CRP ASCM 04 0015, FDR HAVL-argile (available on CD-rom).
6. Poyet, S. (2009). Experimental investigation of the effect of temperature on the first desorption isotherm of concrete. *Cement and Concrete Research*, 39(11), 1052–1059. <https://doi.org/10.1016/j.cemconres.2009.06.019>
7. Yurtdas, I., Burlion, N., Skoczylas, F. (2004). Triaxial mechanical behaviour of mortar: Effects of drying. *Cement and Concrete Research*, 34(7), 1131–1143. <https://doi.org/10.1016/j.cemconres.2003.12.004>
8. Burlion, N., Bourgeois, F., Shao, J. F. (2005). Effects of desiccation on mechanical behaviour of concrete. *Cement and Concrete Composites*, 27, 367–379. <https://doi.org/10.1016/j.cemconcomp.2004.05.004>
9. Bartlett, F. M., MacGregor, J. G. (1994). Effect of moisture condition on concrete core strengths. *ACI Materials Journal*, 91, 227–236.
10. Okajima, T., Ishikawa, T., Ishise, K. (1980). Moisture effect on the mechanical properties of cement mortar. *Transaction of Japan Concrete Institute*, 2, 125–132.
11. Pihlajavaara, S. E. (1974). A review of some of the main results of the research of the ageing phenomena of concrete, effects of moisture conditions of strength, shrinkage and creep of mature concrete. *Cement and Concrete Research*, 4, 761–771. [https://doi.org/10.1016/0008-8846\(74\)90048-9](https://doi.org/10.1016/0008-8846(74)90048-9)
12. Neville, A. M. (2011). *Properties of concrete*. USA: Pearson.
13. Poon, C. S., Azhar, S., Anson, M., Wong, Y. L. (2001). Comparison of the strength and durability performance of normal-and high-strength pozzolanic concretes at elevated temperatures. *Cement and Concrete Research*, 31, 1291–1300. [https://doi.org/10.1016/S0008-8846\(01\)00580-4](https://doi.org/10.1016/S0008-8846(01)00580-4)
14. Poon, C. S., Azhar, S., Anson, M., Wong, Y. L. (2003). Performance of metakaolin concrete at elevated temperatures. *Cement and Concrete Composites*, 25, 83–89. [https://doi.org/10.1016/S0958-9465\(01\)00061-0](https://doi.org/10.1016/S0958-9465(01)00061-0)
15. Dejong, M. J., Ulm, F. J. (2007). The nanogranular behavior of c-s-h at elevated temperatures (up to 700°C). *Cement and Concrete Research*, 37, 1–12. <https://doi.org/10.1016/j.cemconres.2006.09.006>
16. Gaweska, I. (2004). *Thermal behavior of high performance concretes at high temperature-evolution of mechanical properties (Ph.D. Thesis)*. Ecole Nationale des Ponts et Chaussées/Ecole Polytechnique de Cracovie, France.
17. Dilbas, H., Simsek, M., Çakır, Ö. (2014). An investigation on mechanical and physical properties of recycled aggregate concrete (RAC) with and without silica fume. *Construction and Building Materials*, 61, 50–59. <https://doi.org/10.1016/j.conbuildmat.2014.02.057>
18. Chen, G. M., He, Y. H., Yang, H., Chen, J. F., Guo, Y. C. (2014). Compressive behavior of steel fiber reinforced recycled aggregate concrete after exposure to elevated temperatures. *Construction and Building Materials*, 71, 1–15. <https://doi.org/10.1016/j.conbuildmat.2014.08.012>
19. Yonggui, W., Shuaipeng, L., Hughes, P., Yuhui, F. (2020). Mechanical properties and microstructure of basalt fibre and nano-silica reinforced recycled concrete after exposure to elevated temperatures. *Construction and Building Materials*, 247, 118561. <https://doi.org/10.1016/j.conbuildmat.2020.118561>
20. Bazant, Z. P., Raftshol, W. J. (1982). Effect of cracking in drying and shrinkage specimens. *Cement and Concrete Research*, 12, 209–226. [https://doi.org/10.1016/0008-8846\(82\)90008-4](https://doi.org/10.1016/0008-8846(82)90008-4)
21. Sfer, D., Carol, I., Gettu, R., Etse, G. (2002). Study of the behaviour of concrete under triaxial compression. *ASCE Journal of Engineering Mechanics*, 128(2), 156–163. [https://doi.org/10.1061/\(ASCE\)0733-9399\(2002\)128:2\(156\)](https://doi.org/10.1061/(ASCE)0733-9399(2002)128:2(156))
22. Yurtdas, I., Burlion, N., Shao, J. F. (2015). Evolution of mechanical behaviour of mortar with re-saturation after drying. *Materials and Structures*, 48(10), 3343–3355. <https://doi.org/10.1617/s11527-014-0403-7>
23. Malecot, Y., Zingg, L., Briffaut, M., Baroth, J. (2019). Influence of free water on concrete triaxial behavior: The effect of porosity. *Cement and Concrete Research*, 120, 207–216. <https://doi.org/10.1016/j.cemconres.2019.03.010>
24. Wang, Y. Z., Wang, Y. B., Zhao, Y. Z., Li, G. Q., Lyu, Y. F. et al. (2020). Experimental study on ultra-high-performance concrete under triaxial compression. *Construction and Building Materials*, 263, 120225. <https://doi.org/10.1016/j.conbuildmat.2020.120225>

25. Brue, F., Davy, C. A., Skoczylas, F., Burlion, N., Bourbon, X. (2012). Effect of temperature on the water retention properties of two high performance concretes. *Cement and Concrete Research*, 42(2), 384–396. <https://doi.org/10.1016/j.cemconres.2011.11.005>
26. Ranaivomanana, H., Verdier, J., Sellier, A., Bourbon, X. (2011). Toward a better comprehension and modeling of hysteresis cycles in the water sorption–desorption process for cement based materials. *Cement and Concrete Research*, 41, 817–827. <https://doi.org/10.1016/j.cemconres.2011.03.012>
27. Mounanga, P. (2003). *Etude expérimentale du comportement de pâtes de ciment au très jeune âge: Hydratation, retraits, propriétés thermophysiques (Ph.D. Thesis)*. Université de Nantes, France.
28. Huo, J. S., He, Y. M., Xiao, L. P., Chen, B. S. (2013). Experimental study on dynamic behaviours of concrete after exposure to high temperatures up to 700°C. *Materials and Structures*, 46, 255–265. <https://doi.org/10.1617/s11527-012-9899-x>